

Modeling Phase Equilibria and Speciation in Mixed-Solvent Electrolyte Systems¹

P. Wang, R.D. Springer, A. Anderko² and R. D. Young

OLI Systems, Inc., 108 American Road, Morris Plains, NJ 07950, U.S.A.

¹ Paper presented at the 15th Symposium on Thermophysical Properties, June 22-27, 2003, Boulder, Colorado, U.S.A.

² To whom correspondence should be addressed. E-mail: aanderko@olisystems.com.

Abstract

A comprehensive mixed-solvent electrolyte model has been applied to calculate phase equilibria and other thermodynamic properties of multicomponent solutions containing salts, acids and bases in wide concentration ranges. The model combines an excess Gibbs energy model with detailed speciation calculations. The excess Gibbs energy model consists of a long-range interaction contribution represented by the Pitzer-Debye-Hückel expression, a short-range term expressed by the UNIQUAC model and a middle-range term of a second-virial-coefficient type for specific ionic interactions. The model accurately represents the thermodynamic behavior of systems ranging from infinite dilution in water to molten salts or pure acids at temperatures from the freezing point to 300 °C. It has been determined that a physically realistic treatment of speciation is important for the simultaneous representation of vapor-liquid equilibria, osmotic coefficients, solid-liquid equilibria, pH, enthalpies of dilution and heat capacities.

Keywords: Electrolytes, model, excess properties, speciation, solubility, vapor-liquid equilibria

Introduction

Development of models for electrolyte systems is an important subject of research in applied thermodynamics because of the considerable role that electrolytes play in separation processes, environmental applications, production of energy sources, electrochemical processes, hydrometallurgy and other applications. Various models for electrolyte solutions have been recently reviewed by Zemaitis et al. [1], Pitzer [2], Rafal et al. [3], Loehe and Donohue [4] and Anderko et al. [5]. A characteristic feature of electrolyte systems is the fact that phase equilibria and other thermodynamic properties are often inextricably linked to speciation equilibria, which may be due to ion pairing, acid-base reactions, complexation and other phenomena. For many applications, speciation-related properties such as pH, oxidation-reduction potential, distribution of complexed or hydrolyzed species, etc., are of primary importance. Also, speciation can have a significant effect on phase equilibria, such as the solubility of salts in multicomponent systems. Recently, a new thermodynamic model has been developed for the simultaneous computation of speciation, phase equilibria, caloric and volumetric properties of mixed-solvent electrolyte solutions [6]. This model was shown to reproduce the properties of electrolytes in organic or mixed (organic-water) solvents, selected salts from infinite dilution to the fused salt limit and various completely miscible inorganic systems (such as acid-water mixtures) over a full concentration range.

In this study, we apply this model to multicomponent inorganic systems such as those containing two salts and water or a salt, an acid and water in wide concentration ranges that reach the limit of no water. In particular, we focus on systems that are complex because of the formation of multiple hydrated salts, double salts or the presence of eutectic points or congruently melting solid phases. Further, we examine the effect of speciation equilibria on the simultaneous representation of phase equilibria and caloric properties.

Thermodynamic Framework

In a previous paper [6], a thermodynamic framework has been established by combining an excess Gibbs energy model for mixed-solvent electrolyte systems with a comprehensive treatment of chemical equilibria. In this framework, the excess Gibbs energy is expressed as

$$\frac{G^{ex}}{RT} = \frac{G_{LR}^{ex}}{RT} + \frac{G_{MR}^{ex}}{RT} + \frac{G_{SR}^{ex}}{RT} \quad (1)$$

where G_{LR}^{ex} represents the contribution of long-range electrostatic interactions, G_{SR}^{ex} is the short-range contribution resulting from intermolecular interactions, and an additional (middle-range) term G_{MR}^{ex} represents primarily ionic interactions (i.e., ion/ion and ion/molecule) that are not accounted for by the long-range term. The rationale and derivation of eq. (1) was discussed in detail by Wang et al. [6]. Here, we summarize the basic features of the model.

The long-range interaction contribution is calculated from the Pitzer-Debye-Hückel formula [7, 8] expressed in terms of mole fractions and symmetrically normalized, i.e.,

$$\frac{G_{DH}^{ex}}{RT} = - \left(\sum_i n_i \right) \frac{4 A_x I_x}{\rho} \ln \left(\frac{1 + \rho I_x^{1/2}}{\sum_i x_i [1 + \rho (I_{x,i}^0)^{1/2}] } \right) \quad (2)$$

where the sum is over all species, I_x is the mole fraction-based ionic strength, $I_{x,i}^0$ represents the ionic strength when the system composition reduces to a pure component i , i.e., $I_{x,i}^0 = \frac{1}{2} z_i^2$; ρ is related to the hard-core collision diameter ($\rho = 14$) and the A_x parameter is given by

$$A_x = \frac{1}{3} (2\pi N_A d_s)^{1/2} \left(\frac{e^2}{4\pi\epsilon_0\epsilon_s k_B T} \right)^{3/2} \quad (3)$$

where d_s and ϵ_s are the molar density and the dielectric constant of the solvent, respectively. The dielectric constant is calculated from an expression developed previously for mixed solvents [9].

For the short-range interaction contribution, the UNIQUAC equation [10] is used. The middle-range interaction contribution is calculated from an ionic strength-dependent, symmetrical second virial coefficient-type expression [6]:

$$\frac{G_{MR}^{ex}}{RT} = - \left(\sum_i n_i \right) \sum_i \sum_j x_i x_j B_{ij}(I_x) \quad (4)$$

where $B_{ij}(I_x) = B_{ji}(I_x)$, $B_{ii} = B_{jj} = 0$ and the ionic strength dependence of B_{ij} is given by

$$B_{ij}(I_x) = b_{ij} + c_{ij} \exp(-\sqrt{I_x + a_1}) \quad (5)$$

where b_{ij} and c_{ij} are adjustable parameters and a_1 is set equal to 0.01. In general, the parameters b_{ij} and c_{ij} are calculated as functions of temperature as

$$b_{ij} = b_{0,ij} + b_{1,ij}T + b_{2,ij}/T \quad (6)$$

$$c_{ij} = c_{0,ij} + c_{1,ij}T + c_{2,ij}/T \quad (7)$$

In practice, the middle-range parameters are used to represent ion-ion and ion-neutral molecule interaction. The short-range parameters are used primarily for interaction between neutral molecules.

To account for speciation, the chemical effects due to the formation of ion pairs and complexes are explicitly taken into account using chemical equilibria. Also, the same chemical equilibrium formalism is used to calculate solid-liquid equilibria. For this purpose, the standard-state chemical potential μ_i^0 needs to be computed for all species together with the activity coefficients. For solids, the values of μ_i^0 are calculated using the reference-state Gibbs energy of formation, entropy and heat capacity according to standard thermodynamic relationships. For aqueous species, the standard-state chemical potentials are calculated as functions of temperature and pressure using a comprehensive model developed by Helgeson and coworkers (commonly referred to as the Helgeson-Kirkham-Flowers equation of state [11]). The parameters of this model are available for a large number of aqueous species including ions, associated ion pairs, and neutral species [12-15]. It should be noted that standard-state property data and the model of Helgeson et al. are based on the infinite-dilution reference state and on the molality concentration scale. At the same time, the activity coefficient model is symmetrically normalized and is expressed in terms of mole fractions. To make the two reference systems consistent, the activity coefficients calculated from eq. (1) are converted to those based on the unsymmetrical reference state, i.e. at infinite dilution in water, as described by Wang et al. [6]. At the same time, the molality-based standard-state chemical potential is converted to a corresponding mole fraction-based quantity.

A similar procedure is used for enthalpy and heat capacity calculations. In the unsymmetrical normalization, the total enthalpy is expressed as

$$h = \sum_i x_i h_i^* + h^{ex,*} \quad (8)$$

where h_i^* is the standard-state partial molar enthalpy of species i , which can be computed from the Helgeson-Kirkham-Flowers equation and $h^{ex,*}$ is the excess molar enthalpy, which is calculated by differentiating the excess Gibbs energy with respect to temperature and taking into account the change of speciation with temperature [6]. Heat capacities are found by differentiating the enthalpy (eq. 8) with respect to temperature.

Results

The model has been extensively validated using various types of experimental data including vapor-liquid equilibria, osmotic and activity coefficients, solubility of solids, densities, heats of mixing and dilution and various speciation-related data (pH, acid dissociation constants, etc.) In this study, we report selected results obtained for systems containing water and inorganic components, which have

been selected so that the available data extend from dilute aqueous solutions to pure solutes or mixtures without any water.

Figures 1 and 2 show the representation of phase equilibria for the $\text{H}_3\text{PO}_4 + \text{H}_2\text{O}$ mixture, which provides a classical example of a binary system with complex speciation and phase behavior. It was assumed that this system contains the H^+ , PO_4^{3-} , HPO_4^{2-} , H_2PO_4^- and H_3PO_4^0 species. The standard-state properties for these species were calculated from the Helgeson-Kirkham-Flowers equation using the parameters reported by Shock and Helgeson [13]. Although there is some evidence in the literature for the existence of polynuclear phosphorus species in H_3PO_4 , they were not included since they are not necessary for reproducing phase equilibria and pH. Table 1 lists the parameters that were determined to be most significant and were, therefore, adjusted on the basis of experimental data. The parameters shown in Table 1 are defined by eqs. (6) and (7). As shown in Figure 1, the vapor pressure of the $\text{H}_3\text{PO}_4 - \text{H}_2\text{O}$ mixtures is reproduced with good accuracy in the full concentration range. Figure 2 shows the results of calculating the solubility of three solids that may precipitate in this system, i.e., $\text{H}_3\text{PO}_{4(s)}$, $\text{H}_3\text{PO}_4 \cdot 0.5\text{H}_2\text{O}$, and ice. The hydrate $\text{H}_3\text{PO}_4 \cdot 0.5\text{H}_2\text{O}$ forms a congruently melting solid phase, which is accurately reproduced by the model. For calculating the solubilities of the solids, it was necessary to adjust the reference values of the Gibbs energy of formation (ΔG_f^0 (298.15 K)) and entropy (S^0) of the solid phases while using calorimetrically determined heat capacities for these phases. This procedure is generally used since it ensures that solid-liquid equilibria are correctly reproduced in wide temperature ranges together with other properties that are influenced only by liquid-phase parameters (such as VLE, pH or heats of dilution).

One of the most important features of a thermodynamic model is its ability to predict the properties of complex, multicomponent systems using parameters derived from experimental data for simpler (usually binary) systems. To examine the predictive character of the new model, calculations have been performed for sodium and potassium phosphates. Figure 3 shows the calculated solubilities in the binary systems $\text{NaH}_2\text{PO}_4 - \text{H}_2\text{O}$ and $\text{Na}_2\text{HPO}_4 - \text{H}_2\text{O}$. Figure 4 shows analogous solubility relationships for potassium salts. In both cases, the model parameters were determined using VLE and caloric data as well as solubility data. Then, the parameters were used to predict the solubilities in the mixed system $\text{NaH}_2\text{PO}_4 - \text{KH}_2\text{PO}_4 - \text{H}_2\text{O}$. As shown in Figure 5, the solubilities in this system are predicted essentially within the scattering of experimental data.

The model is also capable of reproducing solubilities in systems in which water is not the dominant solvent or is absent altogether. An example of such a system is shown in Figure 6, which illustrates the solubility of FeSO_4 in $\text{H}_2\text{SO}_4 - \text{H}_2\text{O}$ mixtures ranging from pure water to pure sulfuric acid. In this case, the SLE behavior is quite complex with a solubility maximum in concentrated H_2SO_4 solutions and various hydrated forms of FeSO_4 , which precipitate depending on the H_2SO_4 content of the solutions. Figure 7 shows the calculated and experimental solubilities in the ternary system $(\text{NH}_4)_2\text{SO}_4 - \text{H}_2\text{SO}_4 - \text{H}_2\text{O}$ over a substantial temperature range. In contrast to the $\text{FeSO}_4 - \text{H}_2\text{SO}_4 - \text{H}_2\text{O}$ system, an increase in the H_2SO_4 concentration does not drastically reduce the solubility of the salt. However, the solubility behavior is very complex with $(\text{NH}_4)_2\text{SO}_{4(s)}$ precipitating in water-dominated solutions, $\text{NH}_4\text{HSO}_{4(s)}$ precipitating in sulfuric acid-dominated solutions and a double salt $(\text{NH}_4)_2\text{SO}_4 \cdot \text{NH}_4\text{HSO}_{4(s)}$ forming at intermediate concentrations. These phenomena are accurately reproduced by the model.

It is also of interest to analyze the effect of speciation on the computation of thermodynamic properties. In the case of systems such as $\text{H}_3\text{PO}_4 - \text{H}_2\text{O}$ or various weak electrolytes, there is an obvious need to take into account various species that are in chemical equilibrium. However, the

properties of many electrolyte systems can often be reproduced equally well with or without explicitly treating speciation [5]. At the same time, it is well known that strong electrolytes become predominantly ion-paired at high temperatures [16]. Although the applicability range of this model does not extend to the temperatures at which salts become primarily ion-paired (i.e., above ca. 300 °C), a correct limiting behavior at high temperatures should be expected. To investigate this, calculations have been performed for several strong electrolytes by either including or excluding the ion pairs. The KOH – H₂O system has been selected as an example. The calculations have revealed that all properties, except heat capacity, can be reproduced with identical accuracy with or without the KOH⁰ species. This is shown in Figures 8 through 11 for vapor pressures, osmotic coefficients, heats of dilution and solid solubilities. However, the parameters determined from these properties can predict the heat capacity above 200 °C only when the KOH⁰ species is included. This is shown in Figure 12. The solid lines are the predictions when the KOH⁰ species is included while the dashed line at 300 °C represents the predictions when it is not included. The dramatic effect of including the ion pair is evident only well above 200 °C. At such temperatures, the contribution of the ion pair to heat capacity overwhelms the contribution of ions. If the ion pair is neglected, the predicted heat capacities may even become negative (which is physically unrealistic) because the increasingly negative contributions of standard-state properties of individual ions (cf. eq. 8 after differentiating with respect to temperature) cannot be compensated by the positive contribution of the solution nonideality. When the KOH⁰ ion pair is taken into account, all properties can be accurately represented at temperatures up to 300 °C.

Conclusions

A recently developed mixed-solvent electrolyte model has been applied to calculate phase equilibria and other thermodynamic properties of multicomponent solutions containing salts, acids and bases in very wide concentration ranges. The model combines an excess Gibbs energy formulation with comprehensive speciation calculations. It accurately represents multiple properties including vapor-liquid equilibria, osmotic coefficients, solid-liquid equilibria, enthalpies of dilution, heat capacities and pH. The model is valid for aqueous systems ranging from infinite dilution to molten salts or pure acids at temperatures from the freezing point to 300 °C. In particular, the model has been shown to be very useful for reproducing complex solid-liquid equilibrium diagrams, which may involve multiple hydrates, eutectic points formed by salt hydrates and ice, double salts, congruently melting solid phases, etc. It has been determined that the treatment of speciation plays an important role for the simultaneous representation of various properties. For example, phase equilibria for typical strong electrolytes can be reproduced with or without taking into account the formation of ion pairs, which increases in importance as temperature rises. However, a physically reasonable treatment of ion pairing is important for the simultaneous representation of caloric properties and phase equilibria.

Acknowledgments

This work was supported by the Department of Energy under the Cooperative Agreement No DE-FC02-00CH11019 and co-sponsored by Chevron, Dow Chemical, DuPont, MeadWestvaco, Materials Technology Institute, Mitsubishi Chemical, Rohm&Haas and Shell.

References

- [1] J.F. Zemaitis Jr., D.M. Clark, M. Rafal and N.C. Scrivner, Handbook of Aqueous Electrolyte Thermodynamics, DIPPR, AIChE, New York, 1986.
- [2] K.S. Pitzer (ed.), Activity Coefficients in Electrolyte Solutions, 2nd ed., CRC Press, Boca Raton, FL, 1991.
- [3] M. Rafal, J. W. Berthold, N.C. Scrivner and S. L. Grise, Models for Electrolyte Solutions, in Models for Thermodynamic and Phase Equilibria Calculations, S.I. Sandler (ed.), M. Dekker, New York, 1994, p. 601.
- [4] J. R. Loehe, M. D. Donohue, AIChE J., 43 (1997) 180.
- [5] A. Anderko, P. Wang and M. Rafal, Fluid Phase Equilibria, 194-197 (2002) 123.
- [6] P. Wang, A. Anderko and R.D. Young, Fluid Phase Equilibria, 203 (2002) 141.
- [7] K. S. Pitzer, J. Phys. Chem. 77 (1973) 268.
- [8] K. S. Pitzer, J. Am. Chem. Soc. 102 (1980) 2902.
- [9] P. Wang, A. Anderko, Fluid Phase Equil. 186 (2001) 103.
- [10] D. S. Abrams, J. M. Prausnitz, AIChE J. 21 (1975) 116.
- [11] H. C. Helgeson, D. H Kirkham, G.C. Flowers, Amer. J. Sci. 274 (1974) 1089; *ibid.* 274 (1974) 1199; *ibid.* 276 (1976), 97; *ibid.* 281 (1981) 1241.
- [12] E. L. Shock, H. C. Helgeson, D. A. Sverjensky, Geochim. Cosmochim. Acta 53 (1989) 2157.
- [13] E. L. Shock, H. C. Helgeson, Geochim. Cosmochim. Acta 52 (1988) 2009, *ibid.*, 54 (1990) 915.
- [14] E. L. Shock, D. C. Sassani; M. Willis; D. A. Sverjensky, Geochim. Cosmochim. Acta 61 (1997) 907.
- [15] D. A. Sverjensky; E. L. Shock, H. C. Helgeson, *Geochim. Cosmochim. Acta* 61 (1997) 1359.
- [16] A. Anderko and K.S. Pitzer, Geochim. Cosmochim. Acta, 57 (1993) 1657.
- [17] I.A. Kablukov and K.I. Zagwodskin, Z. Anorg. Allgem. Chem., 224 (1935), 315.
- [18] G.S. Kasbekar, J. Ind. Chem. Soc., 17 (1940) 657.
- [19] D.I. MacDonald and J.R. Boyack, J. Chem. Eng. Data, 14 (1969) 380.
- [20] W.H. Ross and R.M. Jones, J. Amer. Chem. Soc., 47 (1925) 2165.
- [21] A. Smith and A.W.C. Menzies, J. Amer. Chem. Soc., 31 (1909) 1183.
- [22] G. Grube and M. Staesche, Z. Phys. Chem., 130 (1927) 572.
- [23] W. Linke, A. Seidell, Solubilities of Inorganic and Metal-Organic Compounds. Vols. 1 and 2, American Chemical Society, Washington, D. C., 1965
- [24] L. Selva, Bull. Soc. Chim. France (1947) 261
- [25] W.L. Marshall, C.E. Hall and R.E. Mesmer, J. Inorg. Nucl. Chem. 43 (1981) 449.
- [26] A.M. Babenko and T.A. Vorobieva, Russ. J. Appl. Chem. 48 (1975) 2519.
- [27] G. Brunisholz and M. Bodmer, Helv. Chim. Acta, 46 (1963) 2566.
- [28] Sh. D. Khallieva, Izv. Akad. Nauk Turkm. SSR Ser. Fiz. Tekh. Khim. Geol., 3 (1977) 125.
- [29] H. L. Silcock, Solubilities of Inorganic and Organic Compounds. Pergamon, New York, 1979
- [30] V.P. Mashovets, B.S. Krumgalz, I.A. Dibrov and R.P. Metveeva, Russ. J. Appl. Chem., 38 (1965) 2294.
- [31] Z. Li and K.S. Pitzer, J. Solution Chem., 25 (1996) 813.
- [32] S.U. Pickering, J. Chem. Soc. London, 63 (1893) 141.
- [33] O. Haehnal, J. Prakt. Chem. 148 (1937) 295.
- [34] V.V. Vyazova and A.D. Pelsha, "Handbook of Experimental Solubility Data for Binary Aqueous and Non-Aqueous Systems Containing Group I Elements", Volume 3, 1961.
- [35] D.D. Wagman, W.H. Evans, V.B. Parker, R.H. Schumm, I. Halow, S.M. Bailey, K.L. Churney and R.L. Nuttall, J. Phys. Chem. Ref. Data, 11 (2) (1982).
- [36] L.V. Puchkov, T.A. Baranova and M.E. Lapidus, Russ. J. Appl. Chem., 43 (1970) 463.

Table 1. Model parameters that were adjusted for the system $\text{H}_3\text{PO}_4 - \text{H}_2\text{O}$.

Binary parameters	Parameters for solid species*
$b_0 (\text{H}^+, \text{H}_2\text{PO}_4^-) = 58.4714$ $b_1 (\text{H}^+, \text{H}_2\text{PO}_4^-) = -7.59140\text{e-}2$ $b_2 (\text{H}^+, \text{H}_2\text{PO}_4^-) = -15075.4$ $c_0 (\text{H}^+, \text{H}_2\text{PO}_4^-) = -125.349$ $c_1 (\text{H}^+, \text{H}_2\text{PO}_4^-) = 0.208888$ $c_2 (\text{H}^+, \text{H}_2\text{PO}_4^-) = 28700.0$ $b_0 (\text{H}_3\text{PO}_4^0, \text{H}_2\text{O}) = 3.33585$ $b_1 (\text{H}_3\text{PO}_4^0, \text{H}_2\text{O}) = -0.48076\text{e-}2$ $b_2 (\text{H}_3\text{PO}_4^0, \text{H}_2\text{O}) = 3182.88$ $c_0 (\text{H}_3\text{PO}_4^0, \text{H}_2\text{O}) = -9.37084$ $c_1 (\text{H}_3\text{PO}_4^0, \text{H}_2\text{O}) = 1.55445\text{e-}2$ $c_2 (\text{H}_3\text{PO}_4^0, \text{H}_2\text{O}) = -196.537$	$\Delta G_f^0 (\text{H}_3\text{PO}_{4(\text{s})}) = -267518.2$ $S^0 (\text{H}_3\text{PO}_{4(\text{s})}) = 25.4659$ $\Delta G_f^0 (\text{H}_3\text{PO}_4 \cdot 0.5\text{H}_2\text{O}) = -297124.8$ $S^0 (\text{H}_3\text{PO}_{4(\text{s})} \cdot 0.5\text{H}_2\text{O}) = 32.1535$

* ΔG_f^0 values are in cal/mol; S^0 values are in cal/(K·mol)

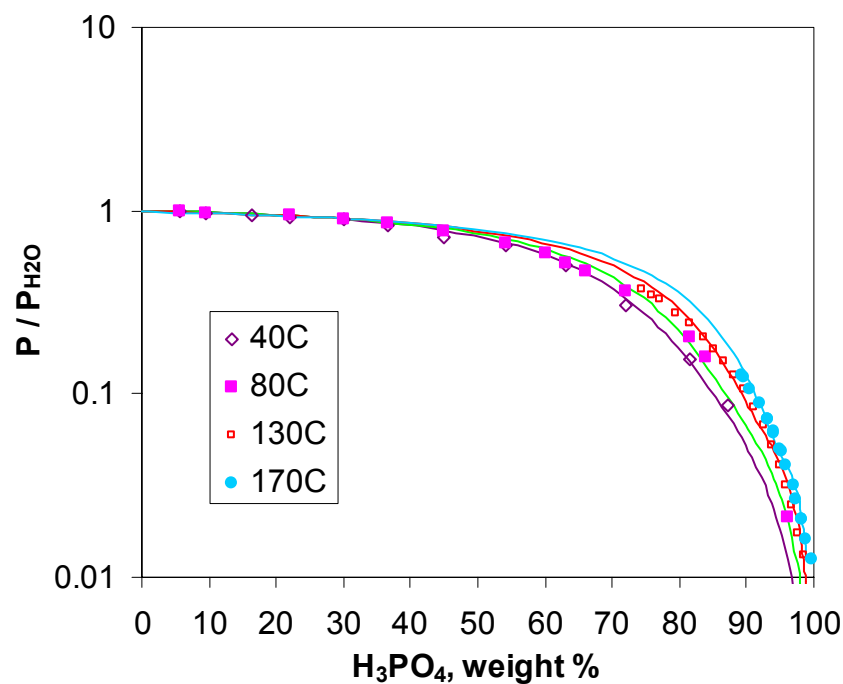


Figure 1. Calculated and experimental vapor pressures in the $H_3PO_4 - H_2O$ system. The symbols represent the data of Kablukov and Zagvosdskii [17], Kasbekar [18] and Macdonald and Boyack [19].

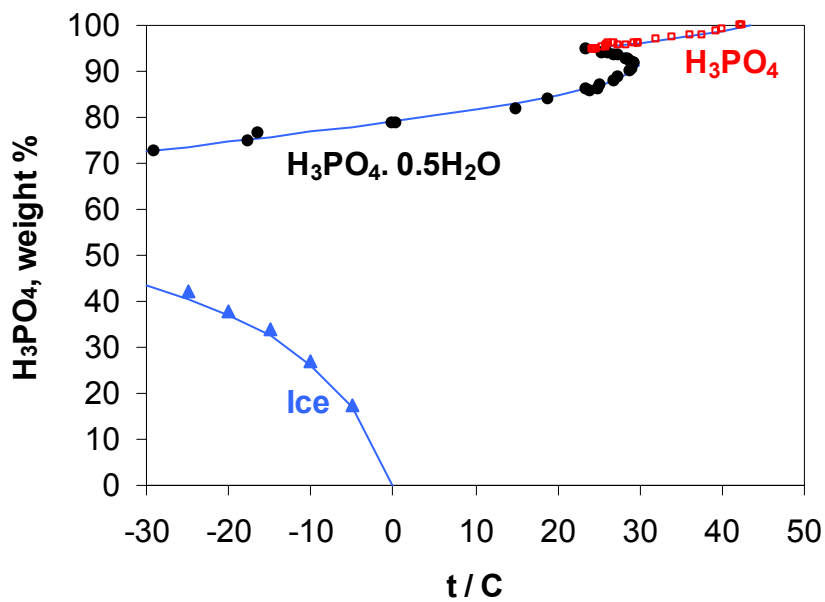


Figure 2. Calculated and experimental solubilities of solids in the $H_3PO_4 - H_2O$ system. The symbols show the data of Ross and Jones [20], Smith and Menzies [21] and Grube and Staesche [22].

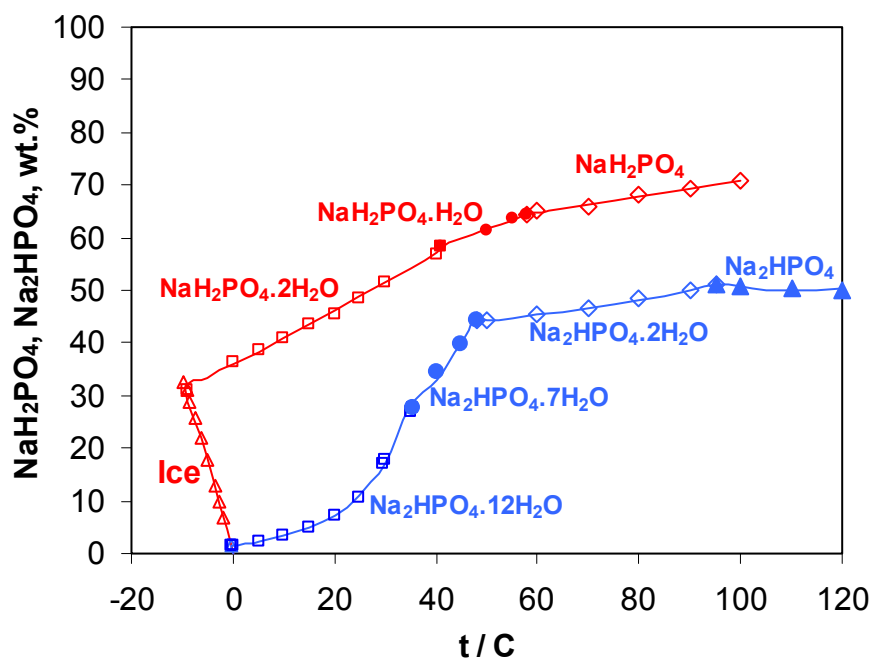


Figure 3. Calculated and experimental solubilities of solids in the binary systems $\text{NaH}_2\text{PO}_4 + \text{H}_2\text{O}$ and $\text{Na}_2\text{HPO}_4 + \text{H}_2\text{O}$. The symbols denote data taken from Linke and Seidell [23].

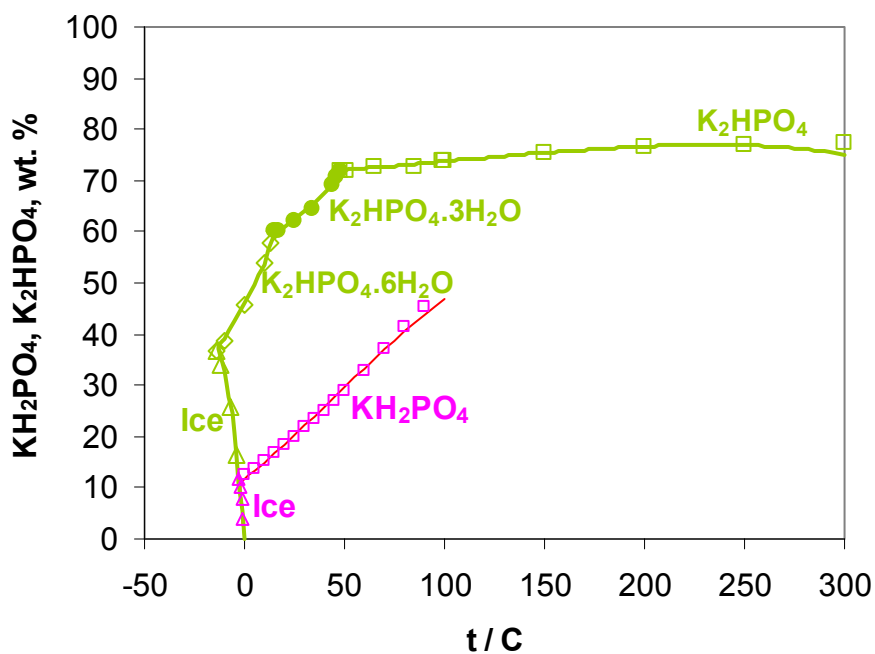


Figure 4. Calculated and experimental solubilities of solids in the binary systems $\text{KH}_2\text{PO}_4 + \text{H}_2\text{O}$ and $\text{K}_2\text{HPO}_4 + \text{H}_2\text{O}$. The symbols represent data taken from Linke and Seidell [23], Selva [24] and Marshall et al. [25].

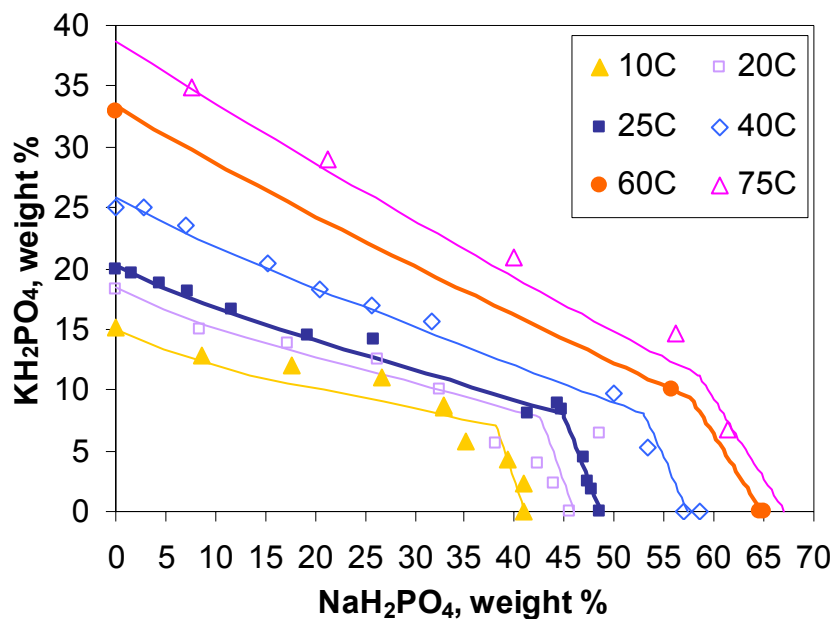


Figure 5. Prediction of solubilities in the system $\text{NaH}_2\text{PO}_4 + \text{KH}_2\text{PO}_4 + \text{H}_2\text{O}$. The symbols denote experimental data from Babenko and Vorobeve [26], Linke and Seidell [24], Brunisholz and Bodmer [27] and Khallieva [28].

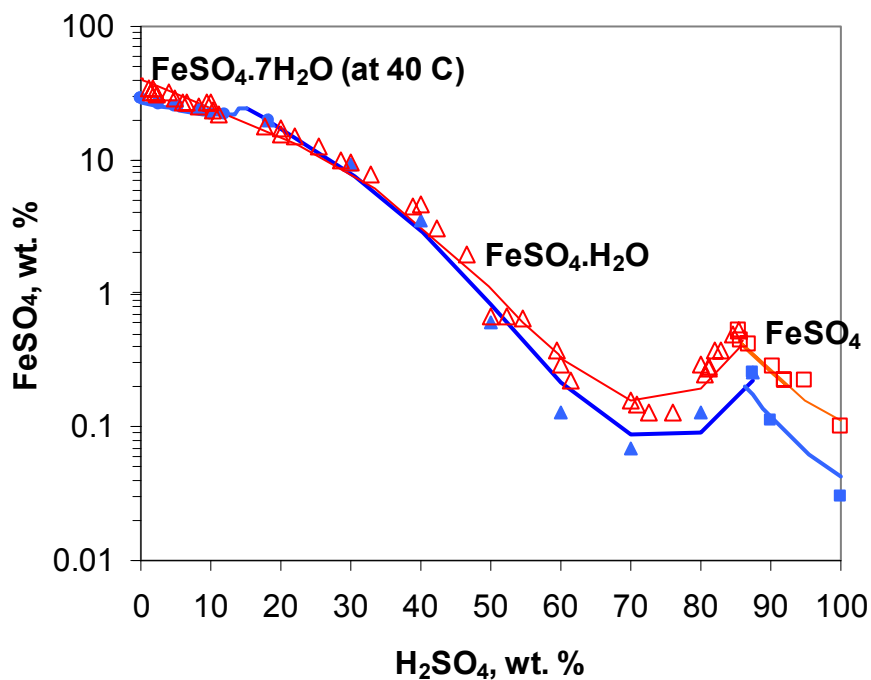


Figure 6. Calculated and experimental solubilities of FeSO_4 in $\text{H}_2\text{SO}_4 + \text{H}_2\text{O}$ mixtures at 40 °C (lower lines) and 60 °C (upper lines). The symbols represent experimental data from Linke and Seidell [24] and Silcock [29].

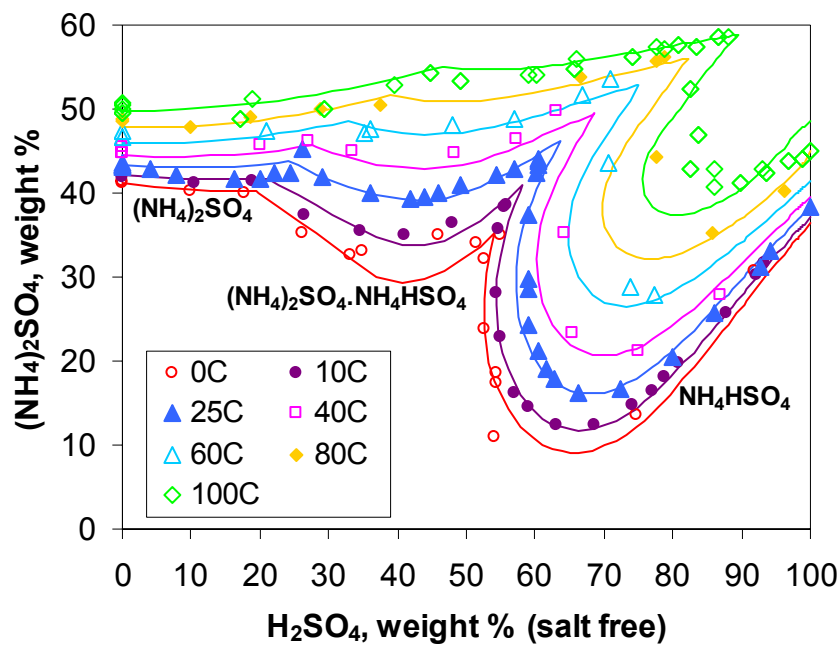


Figure 7. Calculated and experimental solubilities in the system $(\text{NH}_4)_2\text{SO}_4 + \text{H}_2\text{SO}_4 + \text{H}_2\text{O}$. The symbols denote experimental data from Linke and Seidell [24].

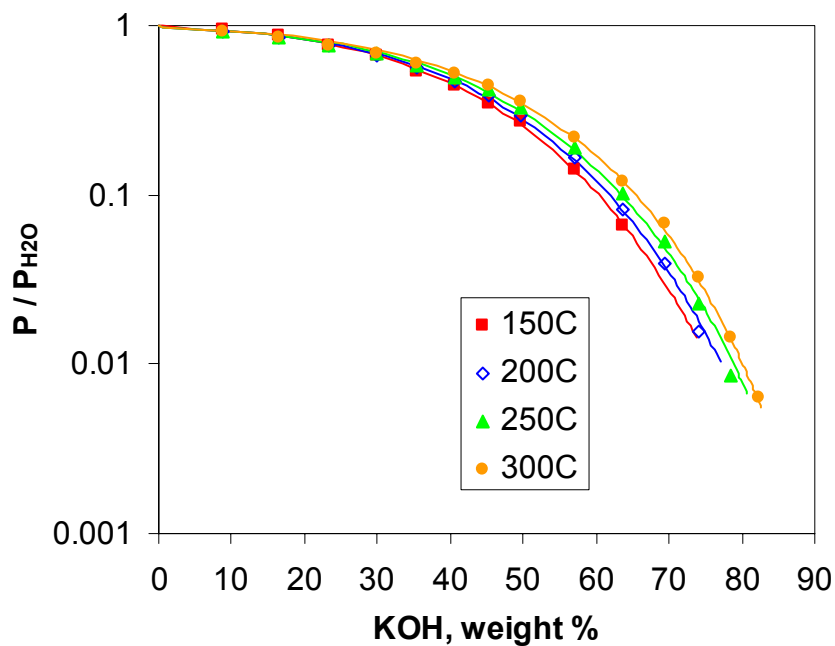


Figure 8. Calculated and experimental vapor-liquid equilibria in the system $\text{KOH}-\text{H}_2\text{O}$. The experimental data are from Mashovets et al. [30].

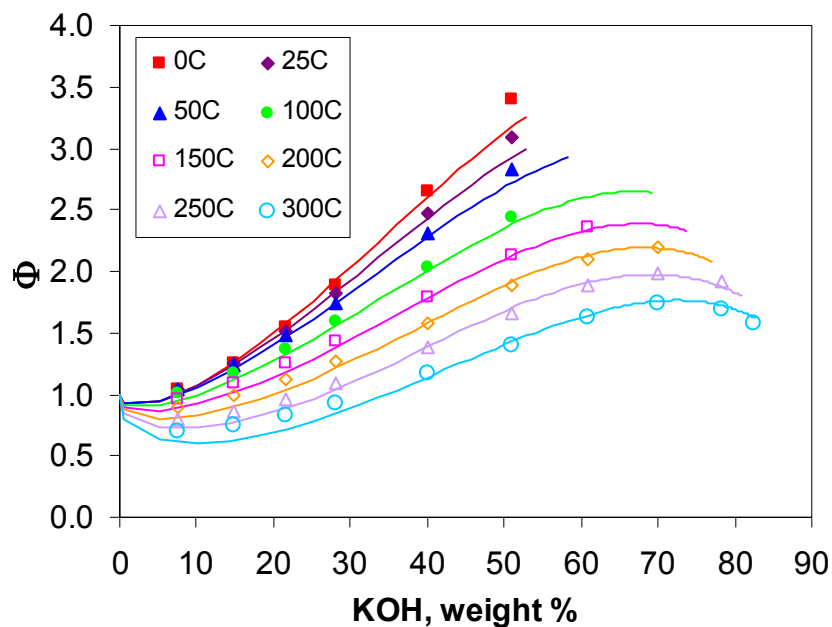


Figure 9. Calculated and experimental osmotic coefficients in the system $\text{KOH}+\text{H}_2\text{O}$. The points denote the values reported by Li and Pitzer [31].

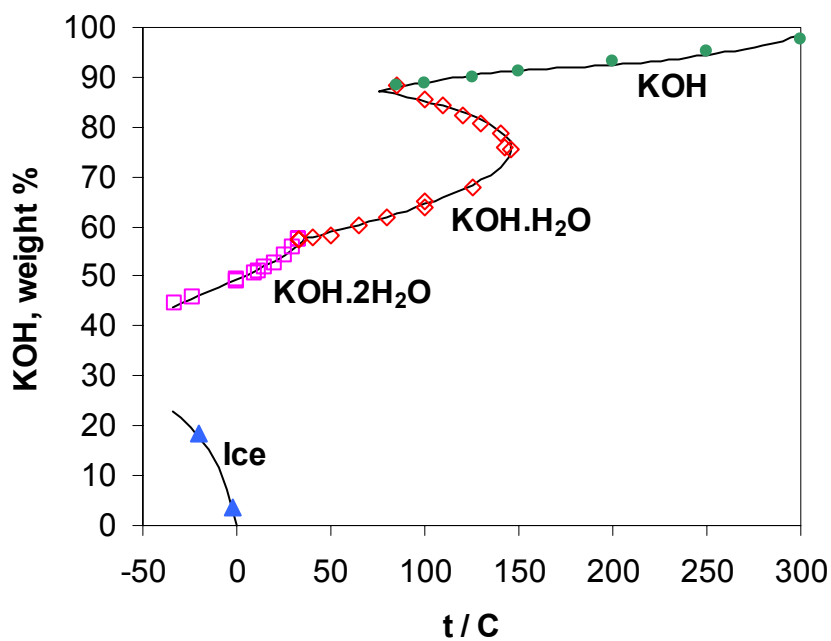


Figure 10. Calculated and experimental solubilities in the system $\text{KOH}+\text{H}_2\text{O}$. The experimental data are from Pickering [32], Haehnel [33] and Vyazova and Pelsha [34].

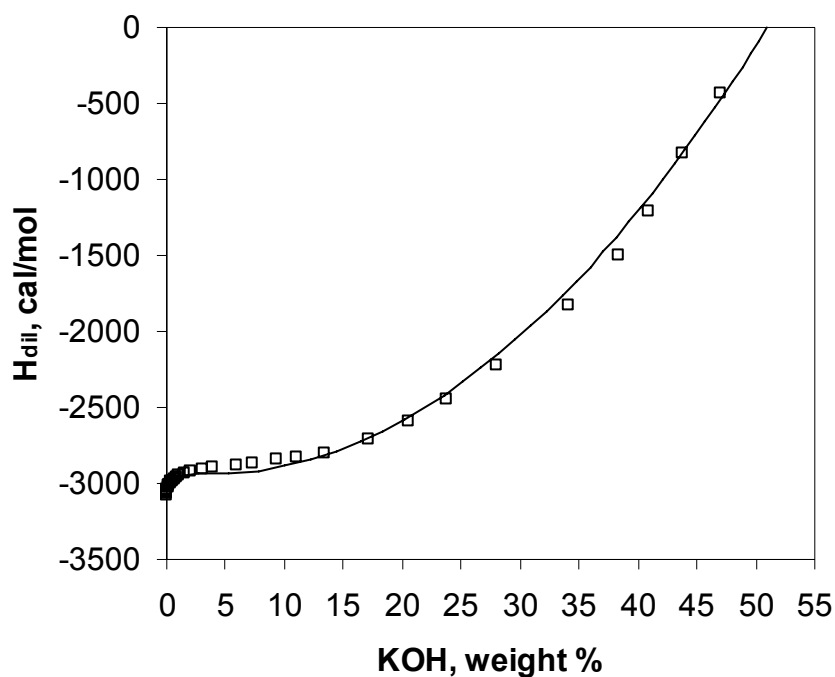


Figure 11. Calculated and experimental enthalpies of dilution in the system KOH+H₂O at 25 °C. The experimental data are from Wagman et al. [35].

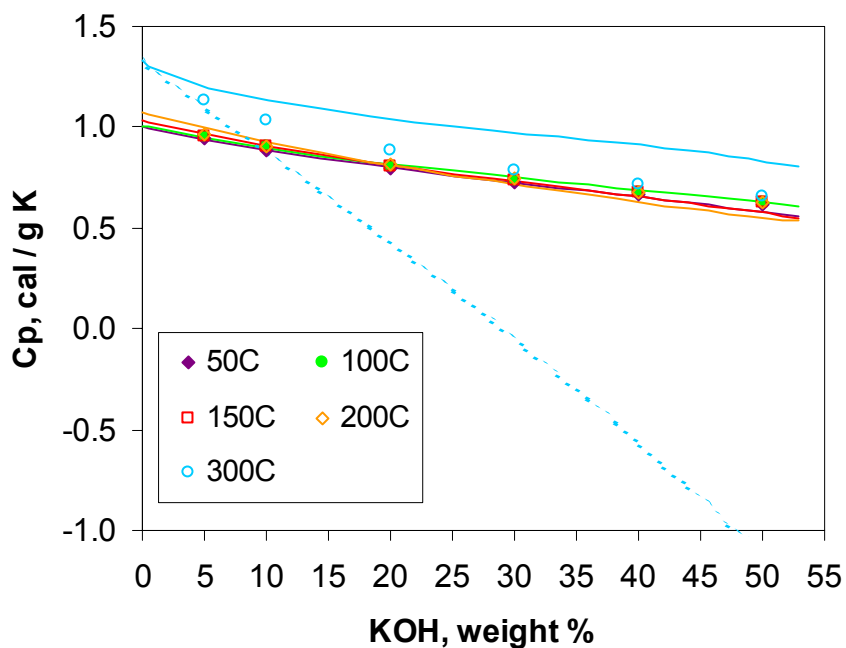


Figure 12. Prediction of heat capacities of KOH+H₂O solutions in cases when the KOH_(aq)⁰ ion pair is included (solid lines) and when it is excluded (dotted line). The dotted line is shown only for 300 °C because the predictions with and without KOH_(aq)⁰ coincide at lower temperatures. The experimental data are from Puchkov et al. [36].